Histol Histopathol (2025) 40: 733-743

Histology and Histopathology
From Cell Biology to Tissue Engineering

ORIGINAL ARTICLE Open Access

Mechanism of KMT2D-mediated epigenetic modification in IL-1β-induced nucleus pulposus cell degeneration

Hongjiang Liu[1], Haiquan Liu[2], Zuyu Meng[3] and Wensheng Zhang[4]

[1]Department of Spine, Third Affiliated Hospital of Guangzhou University of Chinese Medicine, Guangzhou City, [2]Huizhou Hospital of Guangzhou University of Chinese Medicine (Huizhou Hospital of Traditional Chinese Medicine), Huizhou City, [3]College of Chinese Medicine, Jinan University and [4]The Third Affiliated Hospital of Guangzhou University of Chinese Medicine, Guangdong Institute of Traditional Chinese Medicine Bone Injury, Guangzhou City, PR China

Summary. Background. Intervertebral disc (IVD) degeneration (IVDD) is characterized by structural destruction accompanied by accelerated signs of aging. This study aimed to investigate the mechanism of lysine methyltransferase 2D (KMT2D) in the proliferation, apoptosis, and inflammation of nucleus pulposus cells (NPCs) in IVDD.

Methods. Mouse-derived NPCs were cultured and induced with interleukin-1 beta (IL-1β) to establish cell models. KMT2D expression was detected by western blot and reverse transcription-quantitative polymerase chain reaction (RT-qPCR). KMT2D expression was interfered with, and the contents of IL-18, IL-6, and tumor necrosis factor (TNF) were detected by enzyme-linked immunosorbent assay. Cell proliferation, apoptosis, and the expression of miR-133a-5p and 6-phosphofructo-2-kinase/fructose-2,6-biphosphatase 2 (PFKFB2) were measured. The enrichment of KMT2D and Histone 3 Lysine 4 monomethylation/dimethylation (H3K4me1/2) on the miR-133a-5p promoter was analyzed by chromatin immunoprecipitation and qPCR. The binding of miR-133a-5p and PFKFB2 was analyzed by a dual-luciferase assay.

Results. IL-1β treatment promoted KMT2D expression in NPCs. KMT2D knockdown reduced inflammation and apoptosis and promoted the proliferation of IL-1β-induced NPCs. Mechanistically, KMT2D upregulated miR-133a-5p expression by increasing the level of H3K4me2 at the miR-133a-5p promoter, thereby promoting the binding between miR-133a-5p and PFKFB2 and downregulating the transcription of PFKFB2. miR-133a-5p overexpression or PFKFB2 knockdown alleviated the protective effect of KMT2D knockdown on IL-1β-induced NPCs.

Conclusion. KMT2D promoted miR-133a-5p expression through H3K4me2 methylation, thereby promoting the binding of miR-133a-5p to PFKFB2, reducing the mRNA level of PFKFB2, promoting inflammation and apoptosis of IL-1β-induced NPCs, and inhibiting NPC proliferation.

Key words: Intervertebral disc degeneration, Nucleus pulposus cells, KMT2D, miR-133a-5p, PFKFB2

Corresponding Author: Hongjiang Liu, Department of Spine, Third Affiliated Hospital of Guangzhou University of Chinese Medicine, No. 261 Longxi Avenue, Liwan District, Guangzhou City, Guangdong Province, 510000, China. e-mail: liuhongjiang19@163.com
www.hh.um.es. DOI: 10.14670/HH-18-813

Introduction

The incidence of low back pain caused by intervertebral disc (IVD) degeneration (IVDD) is increasing worldwide and it is one of the main causes of disability (Kos et al., 2019; Wu et al., 2020). The intervertebral disc is the soft tissue between the vertebrae that absorbs and distributes the applied load and gives the spine flexibility; IVDD may initiate from biomechanical impairment and disturbed physiological cellular phenotypes, including elevated levels of inflammatory cytokines and enhanced degradation of aggrecan and collagen (Risbud and Shapiro, 2014). In addition, IVDD may also cause IVD herniation and spinal canal stenosis, while senescence and apoptosis of nucleus pulposus cells (NPCs) are the main pathological changes during IVDD (Xin et al., 2022). NPCs are the gelatinous central part of the IVD and are mainly composed of water, proteoglycans, and collagen II (Molladavoodi et al., 2020). Maintaining the normal structure and function of the extracellular matrix by protecting NPCs has been considered a new therapeutic target, which could balance the mechanical loading capacity of IVDs and repair their physiological function (Zhang et al., 2021). This study aimed to investigate the role and mechanism of NPCs in IVDD, to provide more treatment options.

Histone H3 lysine 4 (H3K4) methylation is a chromatin mark, with its monomethylated, dimethylated,

and trimethylated forms differentially enriched at the promoters, enhancers, and other regulatory sequences (Shen et al., 2014). Lysine methyltransferase 2D (KMT2D) belongs to the H3K4 methyltransferase family and functions as monomethyltransferase and dimethyltransferase. KMT2D is a key epigenetic regulator, and the epigenetic regulation mechanism plays an important role in gene expression (Froimchuk et al., 2017). Several studies have reported the role of KMT2D through epigenetic mechanisms in various diseases, such as human congenital heart disease (Ang et al., 2016), fatty liver (Kim et al., 2016), and kabuki syndrome (Boniel et al., 2021). More importantly, KMTD2 is significantly upregulated in severely degenerated IVD through H_2O_2-induced production of reactive oxygen species (Xu et al., 2020). However, the role of KMT2D in NPC degeneration through epigenetic mechanisms remains unclear.

MicroRNAs (miRNAs) are small non-coding RNAs that regulate cell growth, differentiation, development, and apoptosis, thus playing a role in gene regulation, epigenetics, and biological functions (Saliminejad et al., 2019). Previous studies have shown that the expression of miRNAs is epigenetically regulated through DNA methylation, histone modifications, and non-coding RNA regulation (Sato et al., 2011; Piletic and Kunej, 2016). A recent study reported that there is significant methylation modification on the miR-133a promoter histone (Kim et al., 2014). miR-133a-5p was upregulated in seven patients with degenerative lumbar spine diseases (Ishida et al., 2023). Nevertheless, the role of miR-133a-5p in NPCs of IVDD through KMT2D modification has not been reported.

Database prediction and intersection identified that 6-phosphofructo-2-kinase/fructose-2,6-biphosphatase 2 (*PFKFB2*) was the downstream target gene of miR-133a-5p. PFKFB2 is a homodimeric bifunctional enzyme that catalyzes fructose 2,6-bisphosphate to control glycolysis (Rider et al., 2004). For instance, activation of PFKFB2 contributes to the production of glycolytic adenosine triphosphate, promotes alveolar regeneration, and repairs aged lung injury (Wang et al., 2023). Meanwhile, a recent study has proven that PFKFB2 was downregulated in IVDD and inhibited by miR-338-3p, leading to decreased glycolysis and activation of oxidative stress in NPCs (Cao et al., 2021). Therefore, the mechanism of PFKFB2 in NPC degeneration in IVDD may be a new therapeutic target.

In our study, we established cell models to investigate the mechanism of KMT2D in NPC degeneration in IVDD through epigenetics, and to find a new target for the treatment of IVDD.

Materials and methods

Ethics statement

Animal experiments were carried out in strict accordance with the Guide for the Use of Laboratory Animals (Jones-Bolin, 2012). Animal experimental protocols were approved by the Animal Ethics Committee of the Third Affiliated Hospital of Guangzhou University of Chinese Medicine (Approval number: 2023-DSFSYYGZ102).

NPC culture

C57BL/6 mice (n=3, three-month-old, male) were purchased from Shanghai SLAC Laboratory Animal Co., Ltd (Shanghai, China). NPCs were isolated from mouse lumbar intervertebral discs. In brief, mice were euthanized with 3% sodium pentobarbital (150 mg/kg), and lumbar vertebrae were isolated under sterile conditions. After the central nucleus pulposus tissues were isolated under a dissecting microscope (only tissue sections specifically identified as nucleus pulposus were used for macroscopic evaluation in this study), the disc tissues were cut into small blocks and then incubated sequentially with 0.25% trypsin and 0.2% collagenase I for 15 min at 37°C. After filtration through a 70-μm filter (542070, Greiner, Shanghai, China), the suspension was centrifuged at 300g for 5 minutes to ensure exclusion of the notochordal cord cells from the cell cultures. Cell precipitations were then transferred to Dulbecco's modified Eagle's medium/F12 medium containing 15% fetal bovine serum in culture vials. After five days of separation, the adherent spindle-shaped cells at the bottom were identified as passage 0 NPCs. When reaching 80-90% confluence, NPCs were dissociated using 0.25% trypsin and further cultured. NPCs at passage 3 were used for each experiment in this study.

NPC identification

NPCs were fixed in 4% paraformaldehyde for 0.5 h, cultured with 0.1% Triton X-100 for an additional 15 min, and subsequently blocked with 2% bovine serum albumin (Sigma-Aldrich, St. Louis, MO, USA) for 1h. After that, the cells were incubated with collagen II antibody (ab34712, Abcam, Cambridge, MA, USA) overnight at 4°C and then exposed to Alexa Fluor® 488-labeled secondary antibody (ab150077, Abcam). After three regimens of washings with phosphate-buffered saline (PBS), the NPCs were dyed with 4',6-diamidino-2-phenylindole and then photographed and observed with a laser confocal microscope (Olympus, Tokyo, Japan).

NPCs were trypsinized and the cell concentration was adjusted to 1×10^9 cells/L. Two tubes (352235, Corning Falcon) were set and 1 mL of cells were added to each tube. To one tube, 100 μL of CD24-PE antibody was added (1:20, ab25494, Abcam), and isotype control was added to the other tube (1:20, ab154450, Abcam). After treatment for 30 min in the dark, 500 μL of PBS containing 10 g/L paraformaldehyde was added to the sample, and the positive expression rate of CD24 in NPCs was measured by flow cytometry (Beckman Coulter, CA, USA). According to the fluorescence

intensity of isotype control, the negative cells were determined, and the positive expression rate of CD24 in NPCs was observed.

NPC treatment

According to a previous study (He et al., 2021), degeneration of NPCs was induced with 10 ng/mL IL-1β treatment for 24h. Equal volumes of PBS (pH 7.4) were added to the NPCs as a control for IL-1β treated NPCs. miR-133a-5p mimics and mimics NC were purchased from GeneChem (Shanghai, China). The specific small interfering RNA (siRNA) of KMT2D or PFKFB2 and its negative control were purchased from RIBOBIO Technology (Guangzhou, China). Transfection was performed using Lipofectamine 2000 (Invitrogen, Carlsbad, CA, USA) according to the manufacturer's protocol. After 48h of transfection, the isolation of total RNA and protein was implemented and the efficiency was identified. siRNA sequences are listed in Table 1.

Cell counting kit-8 (CCK-8)

NPCs were seeded in 96-well plates at 5×10^3 cells per well and cultured at 37°C with 5% CO_2. At the indicated time points, 10 μL of CCK-8 solution (96992, Sigma-Aldrich) was added for 1h incubation, and the optical density value at 450 nm was measured by a microplate reader to show cell proliferation.

Flow cytometry

According to the instructions of the Annexin V-fluoresceine isothiocyanate/propidium iodide (FITC/PI) Apoptosis Detection Kit (CBA059, Merck Drugs & Biotechnology Co., Ltd., Hesse-Darmstadt, Germany), cells were placed in suspension (1×10^6 cells/mL) using 1× Annexin V binding solution, and 100 μL of this cell suspension was stained with 5 μL of Annexin V-FITC and 5 μL of PI for 15 min. After the addition of 400 μL of Annexin V binding solution, the apoptosis of NPCs after staining was detected using a flow cytometer (Beckman Coulter, CA, USA).

Table 1. siRNA sequences.

Gene	Sequences (5'-3')
si-KMT2D-1	SS Sequence: CGU ACU GUG UCA ACA GCA AGA AS Sequence: UUG CUG UUG ACA CAG UAC GGG
si-KMT2D-2	SS Sequence: CGA GAU GGA GAC UGA UAA AGG AS Sequence: UUU AUC AGU CUC CAU CUC GUG
si-KMT2D-3	SS Sequence: GGA AGU CCC UAG AAG UGA AGA AS Sequence: UUC ACU UCU AGG GAC UUC CGG
si-PFKFB2-1	SS Sequence: AGA GUA AGA UUG UCU ACU ACC AS Sequence: UAG UAG ACA AUC UUA CUC UGG
si-PFKFB2-2	SS Sequence: CCU GCA GAC UGU UAC CUA AGU AS Sequence: UUA GGU AAC AGU CUG CAG GAU
si-PFKFB2-3	SS Sequence: GAU UGU UGU UGG AAG ACC ACU AS Sequence: UGG UCU UCC AAC AAC AAU CUG
si-NC	SS Sequence: CGU ACG AGG GAA AGA GCC UGG AS Sequence: UUU AUC ACU UAG UUU AGU GGU

Enzyme-linked immunosorbent assay (ELISA)

NPCs were washed with PBS, then lysed with radioimmunoprecipitation assay (RIPA) solution, centrifuged at 1400g for 20 min, and the supernatant was collected. The levels of tumor necrosis factor (TNF) (ab208348), IL-6 (ab222503), and IL-18 (ab216165) in NPCs were detected by ELISA kits (Abcam).

Chromatin immunoprecipitation-quantitative polymerase chain reaction (ChIP-qPCR)

ChIP-qPCR analysis was conducted using the SimpleChIP® Enzymatic Chromatin IP Kit (Magnetic Beads) (9003, Cell Signaling Technology, Shanghai, China) according to the manufacturer's instructions. The anti-H3K4Me1 (ab176877, Abcam), anti-H3K4Me2 (ab32356, Abcam), anti-KMT2D (ABE1867, Sigma-Aldrich), and anti-immunoglobulin G (IgG) control (ab172730, Abcam) were used for immunoprecipitation. Immunoselected genomic DNA was subjected to RT-PCR using primers targeting the promoter region of the gene. Primer sequences are listed in Table 2.

Bioinformatics

The Targetscan database (http://www.targetscan.org/vert_71/) (Agarwal et al., 2015), miRWalk database (http://mirwalk.umm.uni-heidelberg.de/) (Sticht et al., 2018), miRDB database (https://mirdb.org/index.html) (Chen and Wang, 2020) and RNA22 database (https://cm.jefferson.edu/rna22/Interactive/) (Miranda et al., 2006) were used to predict downstream target genes of miR-133a-5p.

Dual-luciferase assay

The Targetscan database was used to predict the interaction between miR-133a-5p and the 3'untranslated region (3'UTR) of *PFKFB2*. The sequences of *PFKFB2* 3'UTR wild-type (WT) and mutant (MUT) were constructed by GenScript (Nanjing, Jiangsu, China). miR-133a-5p mimics and *PFKFB2* 3'UTR (WT) or *PFKFB2* 3'UTR (MUT) were transfected using Lipofectamine 2000 (Invitrogen). After 48h, luciferase activity was assessed using a dual-luciferase reporter assay system (Promega Corporation, Madison, WI, USA).

RT-qPCR

Total RNA was extracted from NPCs in each group using the TRIzol method (Thermo Fisher Scientific Inc., Waltham, MA, USA), and the concentration and purity

of RNA were determined. Samples were processed on an Eppendorf PCR amplifier. PCR amplification was performed using SYBR® Premix Ex Taq (DRR041A, TaKaRa Biotech Co., Ltd, Liaoning, China) and an RT-qPCR amplifier (ABI 7500, ABI Company, Oyster Bay, NY), according to the instructions of the PrimeScript RT reagent Kit with gDNA Eraser (RR047B, TaKaRa). U6 (Du et al., 2021) and glyceraldehyde-3-phosphate dehydrogenase (GAPDH) were used as internal parameters, and the $2^{-\Delta\Delta Ct}$ method (Livak and Schmittgen, 2001) was used to measure the fold change.

Western blot (WB) assay

NPCs were incubated in RIPA buffer (400 μL, Cell Signaling Technology) on ice and 100 mM phenyl methyl sulfonyl fluoride was added at a ratio of 10 μL per 1 mL of RIPA buffer, and then centrifuged at 12000 g for 15 min to separate the supernatant. The protein was isolated by 10% sodium dodecyl sulfate-polyacrylamide gel electrophoresis and transferred to a polyvinylidene fluoride membrane (Bio-Rad, Hercules, CA, USA) by electroblotting. The membrane was blocked with 5% skimmed milk powder in Tris-buffered saline with Tween (1× Formulation: 137 mM Sodium Chloride, 20 mM Tris, 0.1% Tween-20. Supplied at pH 7.6; 9997S, Cell Signaling Technology) at room temperature for 1h and then incubated with primary antibodies against KMT2D (PA5-116906, 1:1000, Thermo Fisher Scientific), PFKFB2 (ab241506, 1:2000, Abcam), and β-actin (ab8227, 1:1000, Abcam) at 4°C overnight. Protein bands were probed with goat anti-rabbit IgG (ab205718,

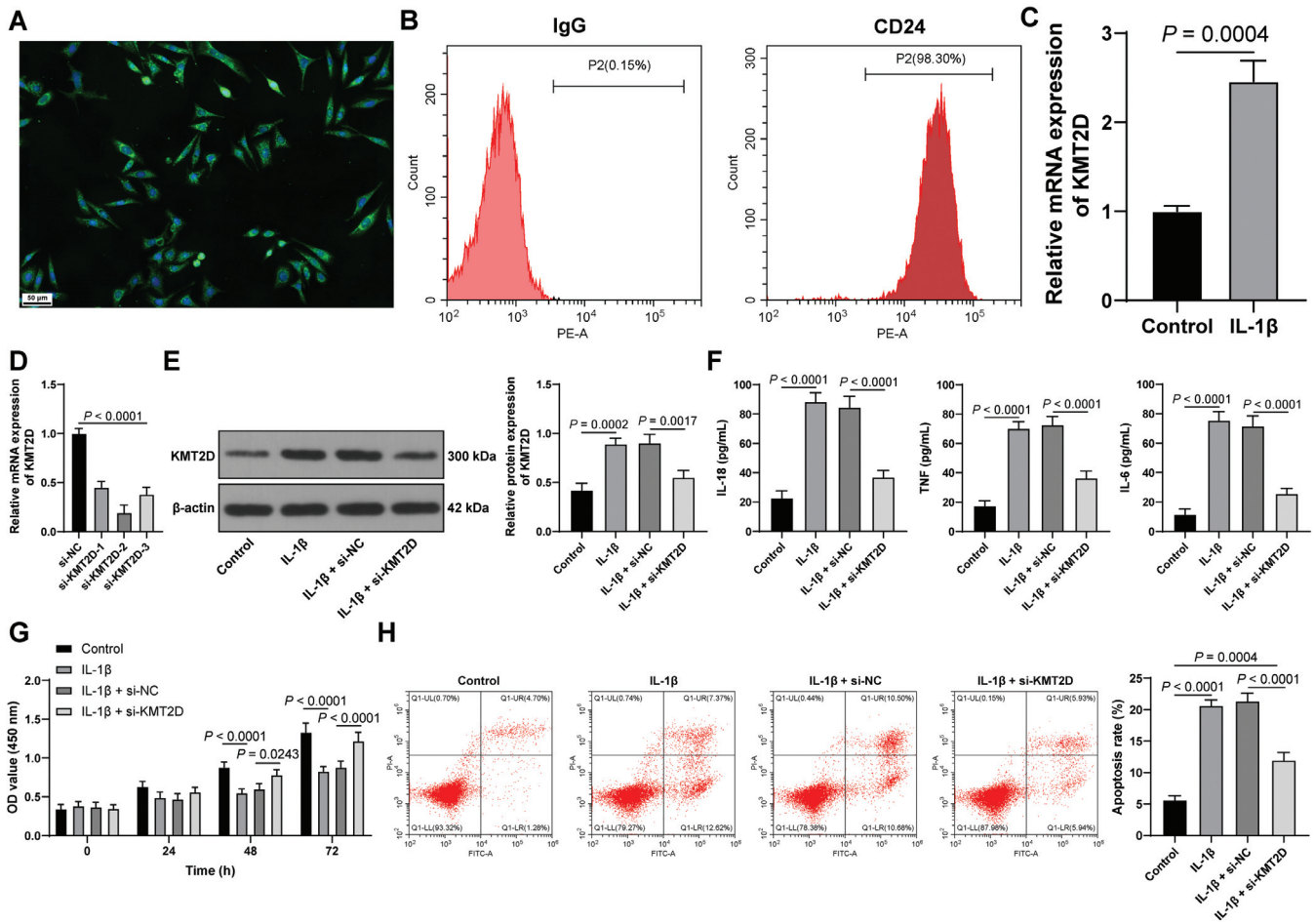

Fig. 1. KMT2D knockdown reduced inflammation, promoted proliferation, and inhibited the apoptosis of IL-1β-treated NPCs. **A.** NPCs in mice were identified using collagen II immunofluorescence staining. **B.** CD24 expression in NPCs of mice was determined using flow cytometry. **C-E.** KMT2D expression in NPCs was detected by RT-qPCR and WB assay. **F.** The levels of IL-18, TNF, and IL-6 in NPCs were detected by ELISA. **G.** CCK-8 was used to detect the proliferation of NPCs. **H.** The apoptosis of NPCs was determined by flow cytometry. Independent experiments were repeated three times, and data are expressed as mean ± SD. Data C: The comparison between two groups was analyzed by *t*-test. Data D-F, and H: comparisons among multiple groups were analyzed by one-way ANOVA. Data G: comparisons among multiple groups were analyzed by two-way ANOVA, followed by Tukey's multiple comparisons post hoc test. mRNA: messenger RNA; IL-1β: interleukin-1 beta; KMT2D: lysine methyltransferase 2D; si-NC: negative control of siRNA; si-KMT2D: KMT2D siRNA; IL-18: interleukin-18; IL-6: interleukin-16; TNF: tumor necrosis factor; OD: optical density; IgG: Immunoglobulin G; WB: Western blot.

1:2000, Abcam) and then detected with enhanced chemiluminescence reagent (Millipore, Billerica, MA, USA). Protein bands were visualized using a LAS-4000 Scientific imaging system (Fuji Film Corporation, Tokyo, Japan), with β-actin antibody as an internal control.

Statistical analysis

SPSS21.0 statistical Software (IBM SPSS Statistics, Chicago, IL, USA) and GraphPad Prism 8.0 Software (GraphPad Software Inc., San Diego, CA, USA) were used for statistical analysis and data mapping. Normality was tested by the Kolmogorov-Smirnov test, which confirmed the normal distribution of data. Data comparison between two groups was analyzed by *t*-test, and data comparisons among multiple groups were analyzed by one-way or two-way analysis of variance (ANOVA), followed by Tukey's multiple comparisons post hoc test. $p<0.05$ was considered statistically significant, and $p<0.01$ was considered extremely statistically significant.

Results

KMT2D knockdown reduced inflammation, promoted proliferation, and inhibited apoptosis of IL-1β-treated NPCs

A study has shown that KMT2D is significantly upregulated in severe IVDD specimens (Xu et al., 2020), however, its role in NPC degeneration of IVD is still unclear. Firstly, NPCs were isolated and cultured *in vitro*. The result of immunofluorescence staining of

Table 2. PCR primer sequences.

Gene	GeneID	Full Name	Sequence (5'-3')
miR-133a-5p	387151	microRNA-133a-5p	F: CGC GTA GGG CTG GTA AAA TGG A R: CAA CTG GTG TCG TGG AGT CGG C
U6	19862	U6 small nuclear RNA	F: CGC TTC GGC AGC ACA TAT ACT R: CTT CAC GAA TTT GCG TGT CAT
KMT2D	381022	lysine methyltransferase 2D	F: ATC AAA CAG GGT CGG AGC AG R: CCA CCA GTG TCT CAA CGG AA
PFKFB2	18640	6-phosphofructo-2-kinase/fructose-2,6-biphosphatase 2	F: TAA AGG CGC AGA TGA GTT ACC A R: TTC TCC ACT TCA GTT GGC TTG
GAPDH	14433	glyceraldehyde-3-phosphate dehydrogenase	F: GGT CCC AGC TTA GGT TCA TCA R: AAT CCG TTC ACA CCG ACC TT
miR-133a-5p promoter	-	-	F: CAC AGG AAA CTG GGT GAA TGC T R: ACA AGA GGG GAA AAG TTG CAG A

Denaturation was carried out at 95°C for 30 seconds, annealing at 60°C for 30 seconds, and extension at 72°C for 30 seconds, for a total of 39 cycles.

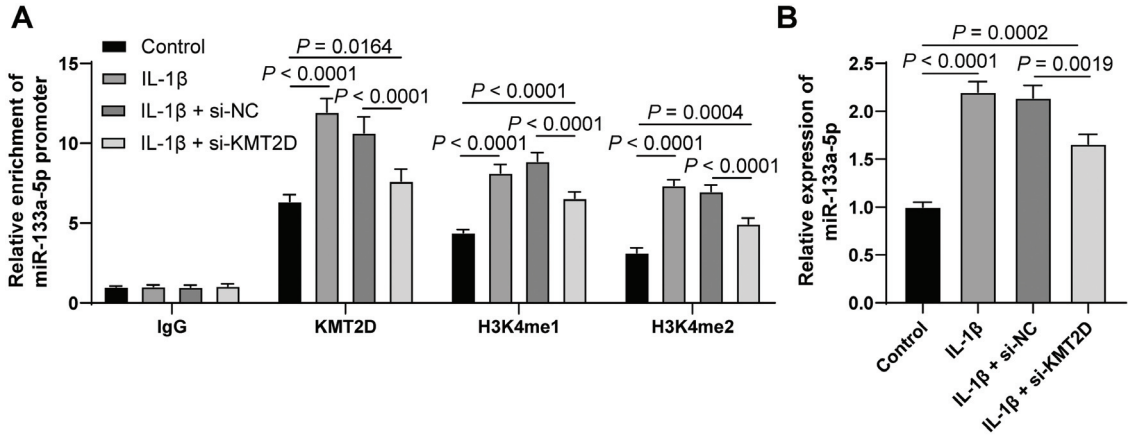

Fig. 2. KMT2D increased the level of H3K4me1/2 on the miR-133a-5p promoter to upregulate miR-133a-5p expression. **A.** The enrichment of KMT2D and H3K4me1/2 on the promoter of miR-133a-5p was analyzed by ChIP. **B.** The expression of miR-133a-5p in NPCs was detected by RT-qPCR. Independent experiments were repeated three times, and data are expressed as mean ± SD. Data A: comparisons among multiple groups were analyzed by two-way ANOVA. Data B: comparisons among multiple groups were analyzed by one-way ANOVA, followed by Tukey's multiple comparisons post hoc test. IL-1β: interleukin-1 beta; KMT2D: lysine methyltransferase 2D; si-NC: negative control of siRNA; si-KMT2D: KMT2D siRNA; IgG: Immunoglobulin G; H3K4me1: histone H3 lysine 4 monomethylation; H3K4me2: histone H3 lysine 4 dimethylation.

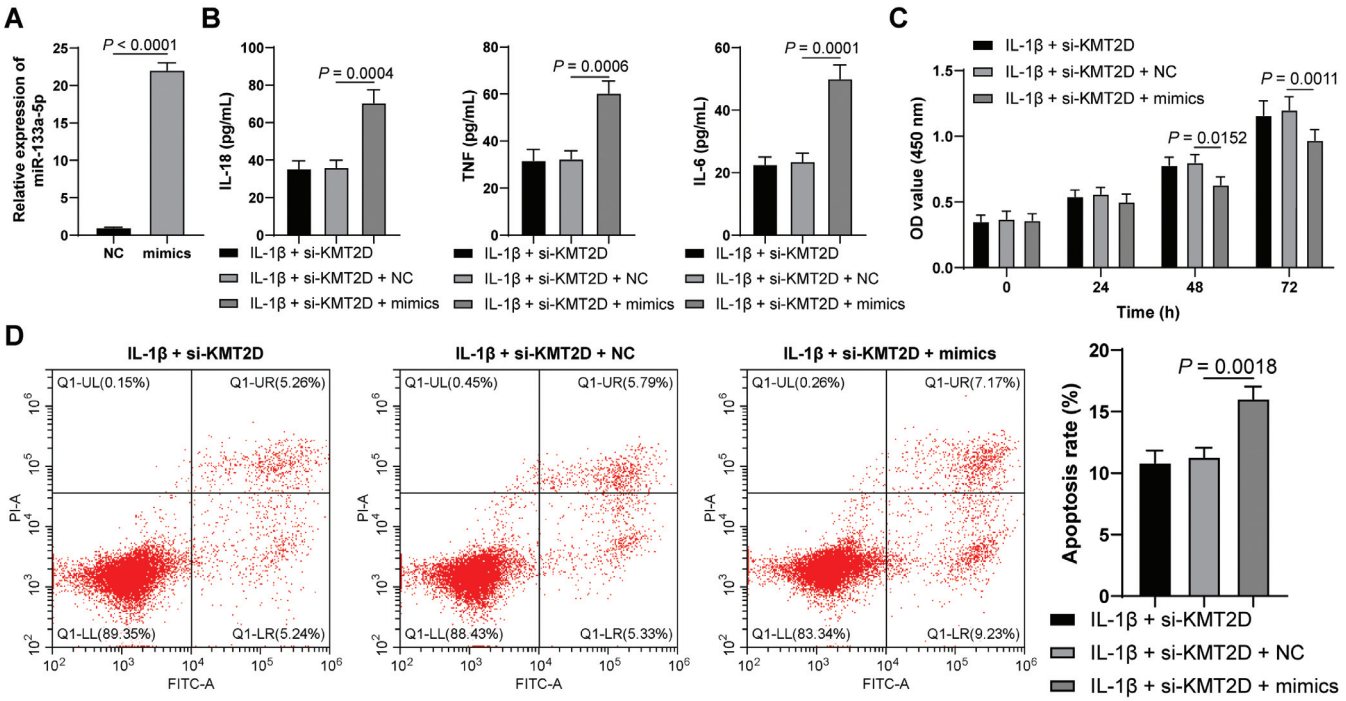

Fig. 3. Overexpression of miR-133a-5p alleviated the protective effect of KMT2D knockdown on nucleus pulposus cell degeneration. Mimics were transfected into NPCs and NC were used as the negative control. **A.** The expression of miR-133a-5p in NPCs was analyzed by RT-qPCR. **B.** The levels of IL-18, TNF, and IL-6 in NPCs were detected by ELISA. **C.** The proliferation of NPCs was detected by CCK-8. **D.** The apoptosis of NPCs was observed by flow cytometry. Independent experiments were repeated three times, and data are expressed as mean ± SD. Data A: The comparison between two groups was analyzed by *t*-test. Data B and D: comparisons among multiple groups were analyzed by one-way ANOVA. Data C: comparisons between multiple groups were analyzed by two-way ANOVA, followed by Tukey's multiple comparisons post hoc test. IL-1β: interleukin-1 beta; KMT2D: lysine methyltransferase 2D; NC: mimics NC; mimics: miR-133a-5p mimics; IL-18: interleukin-18; IL-6: interleukin-16; TNF: tumor necrosis factor; OD: optical density.

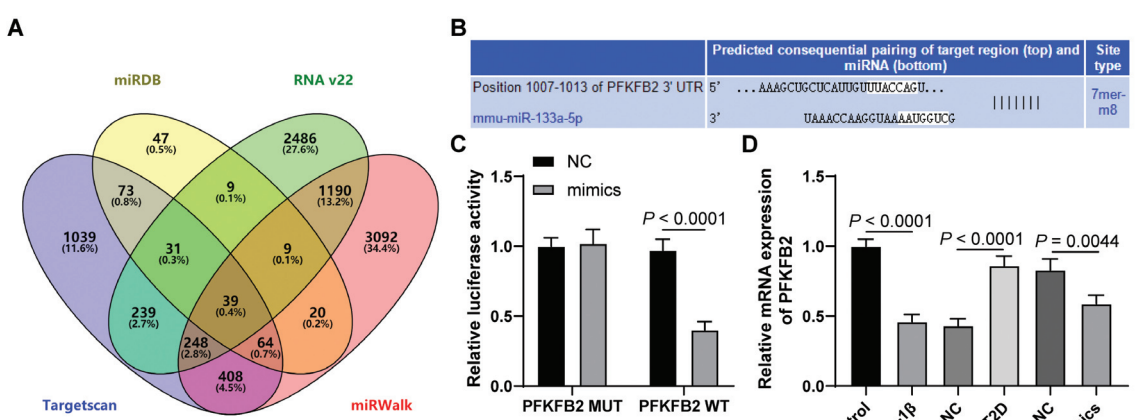

Fig. 4. miR-133a-5p inhibited the transcription level of PFKFB2. **A.** The database predicted the downstream target genes of miR-133a-5p and obtained the intersection. **B.** Binding sites of miR-133a-5p and PFKFB2 in Targetscan database. **C.** The targeted binding of miR-133a-5p and PFKFB2 was analyzed by dual luciferase assay. **D.** The expression of *PFKFB2* in NPCs was detected by RT-qPCR. Independent experiments were repeated three times, and data are expressed as mean ± SD. Data C: comparisons among multiple groups were analyzed by two-way ANOVA. Data D: comparisons among multiple groups were analyzed by one-way ANOVA, followed by Tukey's multiple comparisons post hoc test. mRNA: messenger RNA; IL-1β: interleukin-1 beta; KMT2D: lysine methyltransferase 2D; si-NC: negative control of siRNA; si-KMT2D: KMT2D siRNA; NC: mimics NC; mimics: miR-133a-5p mimics; PFKFB2: 6-phosphofructo-2-kinase/fructose-2,6-biphosphatase 2.

NPCs was positive, indicating an enrichment of collagen II in NPCs (Fig. 1A). Flow cytometry results showed that the expression of CD24 was positive in NPCs *in vitro* (Fig. 1B). Next, NPCs were induced with IL-1β, and the expression of KMT2D was significantly increased in IL-1β-treated NPCs ($p<0.01$, Fig. 1C,D). To verify the effect of KMT2D on IL-1β-treated NPCs, we first transfected KMT2D siRNA (si-KMT2D) into NPCs to reduce the intracellular *KMT2D* mRNA level ($p<0.01$, Fig. 1D). si-KMT2D-2 (si-KMT2D) with better transfection efficiency was selected for subsequent experiments. Following si-KMT2D treatment, a significant reduction in the protein levels of KMT2D induced by IL-1β was observed ($p<0.01$, Fig. 1E). Moreover, the contents of intracellular inflammatory factors IL-18, TNF, and IL-6 were significantly decreased after KMT2D knockdown ($p<0.01$, Fig. 1F). KMT2D knockdown clearly promoted proliferation and inhibited apoptosis of NPCs ($p<0.01$, Fig. 1G,H). These results indicated that KMT2D knockdown could reduce the inflammation, promote the proliferation, and inhibit the apoptosis of IL-1β-treated NPCs.

KMT2D increased the level of H3K4me1/2 on the miR-133a-5p promoter to upregulate miR-133a-5p expression

KMT2D is one of the major monomethyltransferases and dimethyltransferases (H3K4me1 and H3K4me2) (Shinsky et al., 2015). Studies have shown that miR-133a promoter histone has significant methylation modification (Kim et al., 2014), and miR-133a-5p is highly expressed in IVDD tissues (Du et al., 2021). We hypothesized that miR-133a-5p was the downstream target gene of KMT2D. ChIP-qPCR results showed that KMT2D was enriched on the miR-133a-5p promoter, and KMT2D knockdown reduced the enrichment of KMT2D and H3K4me1/2 on the miR-133a-5p promoter ($p<0.01$, Fig. 2A). The expression of miR-133a-5p was detected and it was found that IL-1β treatment promoted the expression of miR-133a-5p, while KMT2D knockdown inhibited its expression ($p<0.01$, Fig. 2B). In conclusion, KMT2D increased H3K4me1/2 levels on the miR-133a-5p promoter to upregulate miR-133a-5p expression.

Overexpression of miR-133a-5p alleviated the protective effect of KMT2D knockdown on NPC degeneration

Then, we transfected NPCs with miR-133a-5p mimics (mimics) to increase the expression of miR-133a-5p in cells ($p<0.01$, Fig. 3A), and combined experiments were performed with si-KMT2D. The results showed that overexpression of miR-133a-5p increased the levels of IL-18, TNF, and IL-6 in IL-1β-treated cells ($p<0.01$, Fig. 3B). In addition, upregulation of miR-133a-5p significantly inhibited the proliferation of NPCs and promoted their apoptosis ($p<0.05$, Fig. 3C,D). These results indicated that overexpression of miR-133a-5p alleviated the protective effect of KMT2D knockdown on NPC degeneration in IVD.

miR-133a-5p inhibited the transcription level of PFKFB2

The downstream target genes of miR-133a-5p were predicted and the intersections were obtained (Fig. 4A) from miRDB databases, RNA v22, Targetscan database, and miRWalk database. A total of 39 genes were found in the intersection (Table 3). Among them, *PFKFB2* was poorly expressed in IVDD (Cao et al., 2021), thus *PFKFB2* was selected as the study object. Dual-luciferase assay confirmed the binding between miR-133a-5p and PFKFB2 in NPCs ($p<0.01$, Fig. 4B,C). The transcriptional level of *PFKFB2* was detected, and the results showed that the expression of PFKFB2 was decreased by IL-1β treatment, upregulated by downregulation of KMT2D, but reduced again by further overexpression of miR-133a-5p ($p<0.01$, Fig. 4D).

Table 3. 39 common elements in "miRDB", "RNA v22", "Targetscan" and "miRWalk".

miRNA	Target gene
mmu-miR-133a-5p	*CAPRIN1*
mmu-miR-133a-5p	*WNK1*
mmu-miR-133a-5p	*TFG*
mmu-miR-133a-5p	*RNF19B*
mmu-miR-133a-5p	*NOVA1*
mmu-miR-133a-5p	*ONECUT2*
mmu-miR-133a-5p	*CADM2*
mmu-miR-133a-5p	*COL4A5*
mmu-miR-133a-5p	*SLIT2*
mmu-miR-133a-5p	*ELF1*
mmu-miR-133a-5p	*MAN1A2*
mmu-miR-133a-5p	*XRN2*
mmu-miR-133a-5p	*SNX33*
mmu-miR-133a-5p	*NTNG1*
mmu-miR-133a-5p	*NCOA3*
mmu-miR-133a-5p	*SOS1*
mmu-miR-133a-5p	*IPCEF1*
mmu-miR-133a-5p	*HLF*
mmu-miR-133a-5p	*PPFIBP1*
mmu-miR-133a-5p	*ARL2BP*
mmu-miR-133a-5p	*KDM5A*
mmu-miR-133a-5p	*SCN3A*
mmu-miR-133a-5p	*LRAT*
mmu-miR-133a-5p	*VTA1*
mmu-miR-133a-5p	*SH3PXD2B*
mmu-miR-133a-5p	*PPT1*
mmu-miR-133a-5p	*CCDC85A*
mmu-miR-133a-5p	*TSHZ2*
mmu-miR-133a-5p	*NDRG3*
mmu-miR-133a-5p	*SYNRG*
mmu-miR-133a-5p	*SYNE2*
mmu-miR-133a-5p	*ANKRD13A*
mmu-miR-133a-5p	*NDST2*
mmu-miR-133a-5p	*PGAP1*
mmu-miR-133a-5p	*YWHAB*
mmu-miR-133a-5p	*MBTD1*
mmu-miR-133a-5p	*PRRX1*
mmu-miR-133a-5p	*PFKFB2*
mmu-miR-133a-5p	*TLE3*

These results indicated that miR-133a-5p inhibited the transcriptional level of PFKFB2.

Downregulation of PFKFB2 alleviated the protective effect of KMT2D knockdown on NPC degeneration

PFKFB2 siRNA (si-PFKFB2) was transfected into NPCs to reduce the expression of PFKFB2 in cells ($p<0.01$, Fig. 5A,B), and the si-PFKFB2-3 with the best transfection efficiency was selected for combined experiments with si-KMT2D. The results showed that knockdown of PFKFB2 expression upregulated the contents of IL-18, TNF, and IL-6 in IL-1β-treated cells ($p<0.01$, Fig. 5C). In addition, inhibition of PFKFB2 expression significantly inhibited the proliferation and promoted the apoptosis of NPCs ($p<0.01$, Fig. 5D,E). These results suggested that the downregulation of PFKFB2 alleviated the protective effect of KMT2D knockdown on NPC degeneration.

Discussion

Current treatment modalities (medical, surgical, and interventional therapy) for IVDD mainly provide relief, with the possibility of complications (Li et al., 2023). The epigenetic modification affects the pathological process of IVDD through DNA methylation, histone modification, and non-coding RNA regulation, suggesting its possibility as a therapeutic mechanism (Kang et al., 2023). In our study, we found that KMT2D promoted the expression of miR-133a-5p through H3K4me2 methylation on the miR-133a-5p promoter, thereby promoting the binding of miR-133a-5p to PFKFB2 to reduce the mRNA level of PFKFB2, increasing inflammation and apoptosis of IL-1β-treated NPCs, and inhibiting the proliferation of NPCs.

In tissues from patients with degenerative discs, KMT2D-positive NPCs in the severe IVDD group (Grade IV and Grade V) were 4.7-fold higher than those in the mild IVDD group (Grade II and Grade III), indicating the potential role of overexpression of KMT2D in IVDD (Xu et al., 2020). Furthermore, KMT2D expression is upregulated in NPCs of IVDD, which might be induced by oxidative stress, meanwhile, the expression of H3K4me1 and H3K4me2, and the levels of monomethylation and dimethylation are also increased in NPCs of IVDD (Xu et al., 2020), suggesting that KMT2D is involved in IVDD through methylation modification. Extracellular matrix degradation and upregulation of oxidative stress levels and inflammation levels of NPCs are generally found in IVDD (Qi et al., 2020). In addition, the elevation of KMT2D is associated with the release of inflammatory factors and the promotion of apoptosis (Chen et al., 2015). Consistently,

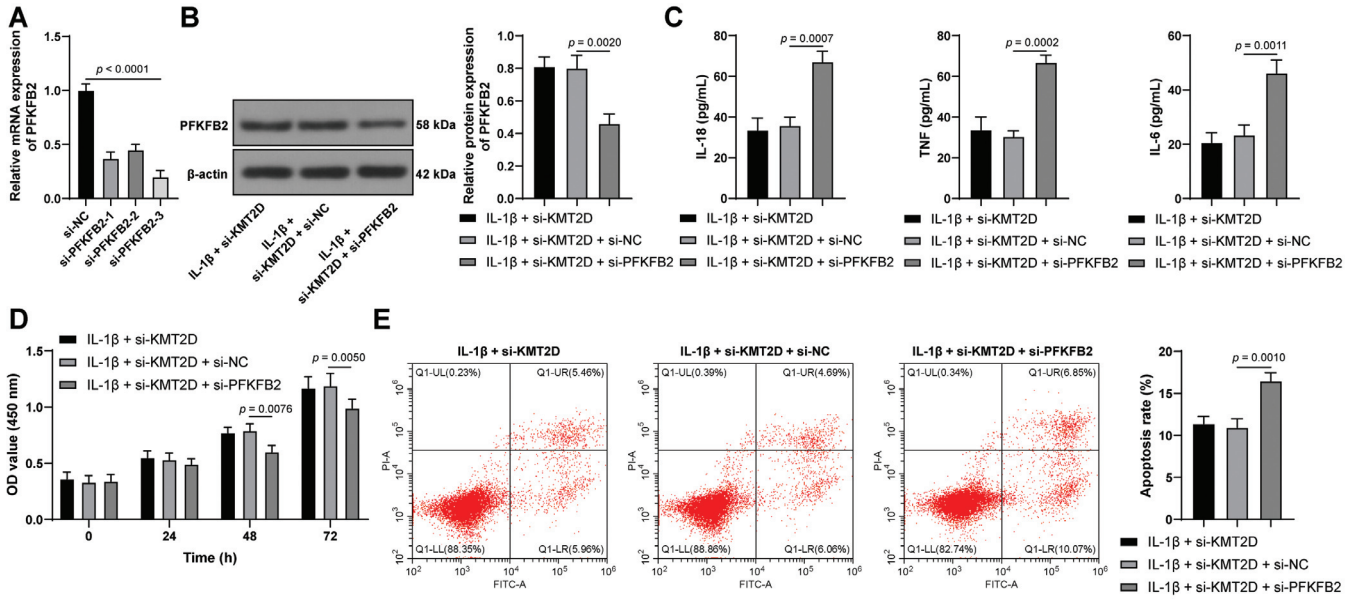

Fig. 5. Downregulation of PFKFB2 alleviated the protective effect of KMT2D knockdown on NPC degeneration. PFKFB2 siRNA (si-PFKFB2) was transfected into NPCs, with si-NC as the negative control. **A, B.** The expression of PFKFB2 in NPCs was analyzed by RT-qPCR and WB assay. **C.** The levels of IL-18, TNF, and IL-6 in NPCs were analyzed by ELISA. **D.** The proliferation of NPCs was detected by CCK-8. **E.** Apoptosis of NPCs was determined by flow cytometry. Independent experiments were repeated three times, and data are expressed as mean ± SD. Data A-C, and E: comparisons among multiple groups were analyzed by one-way ANOVA. Data D: comparisons among multiple groups were analyzed by two-way ANOVA, followed by Tukey's multiple comparisons post hoc test. mRNA: messenger RNA; IL-1β: interleukin-1 beta; KMT2D: lysine methyltransferase 2D; PFKFB2: 6-phosphofructo-2-kinase/fructose-2,6-biphosphatase 2; si-NC: negative control of siRNA; si-KMT2D: KMT2D siRNA; si-PFKFB2: PFKFB2 siRNA; IL-18: interleukin-18; IL-6: interleukin-16; TNF: tumor necrosis factor; OD: optical density; WB: Western blot.

our study confirmed that KMT2D was increased in NPCs, and knockdown of KMT2D significantly reduced the levels of inflammatory factors, promoted cell proliferation, and reduced apoptosis.

Increasing evidence has shown that miRNAs play a role in IVDD. Upregulation of miR-19b-3p promotes the proliferation of human NPCs and inhibits their apoptosis (Zhao and Li, 2021); Exosomal miR-26a-5p reduces cell death and low cell viability of NPCs in IVDD induced by METTL14 degradation (Yuan et al., 2021). miR-133a-5p is enhanced in the inflammatory environment of IVDD, and inhibition of miR-133a-5p increases the expression of aggrecan and collagen II in NPCs (Du et al., 2021). Meanwhile, miR-133a-5p was upregulated in osteoarthritis (Ishida et al., 2023), and IVDD often occurs in tandem with osteoarthritis, which shares similar pathological features with IVDD, such as cartilage destruction, extracellular matrix degeneration, and osteophyte formation, as well as inflammation and extracellular matrix degradation (Francisco et al., 2022; Fine et al., 2023). Therefore, we hypothesized that miR-133a-5p is the downstream target gene of KMT2D, and the ChIP-qPCR results showed that KMT2D was enriched in the promoter of miR-133a-5p. Down-regulation of KMT2D reduced the enrichment of KMT2D and H3K4me1/2 on the miR-133a-5p promoter and inhibited the expression of miR-133a-5p. Furthermore, overexpression of miR-133a-5p increased the levels of inflammatory factors in NPCs, resulting in inhibited proliferation and stimulated apoptosis of NPCs. Interestingly, the proinflammatory effects of miR-133a upregulation had been demonstrated in a previous study (Zhao and Ai, 2020), and miR-133a-3p overexpression could also inhibit the proliferation of intestinal epithelial cells and promote the apoptosis of intestinal epithelial cells (Tian et al., 2021).

Since miR-133a-5p was highly expressed in IVDD, we decided to explore the downstream target genes of miR-133a-5p. The database and dual-luciferase experiment verified a targeted binding relationship between miR-133a-5p and PFKFB2. Low levels of PFKFB2 lead to dysregulation of glycolytic metabolism and increased cellular oxidative stress levels in NPCs (Cao et al., 2021), while glycolysis is the main energy metabolism pathway of NPCs, whose disorder can lead to degeneration and damage to the normal physiological function of NPCs (Wu et al., 2021). Loss of phosphorylation of PFKFB2 exacerbates inflammatory diseases (Bruce et al., 2021). Similarly, we found that PFKFB2 was targeted by miR-133a-5p and down-regulation of PFKFB2 worsened inflammation and damage in NPCs, suggesting an aggravating effect of PFKFB2 downregulation on degeneration of NPCs.

Our study still has some limitations. First, only a single downstream mechanism of KMT2D was explored, and other possible downstream mechanisms were not further investigated. Second, we have only conducted cell experiments, and the mechanism has not been verified or explored at the animal level. Third, there may be other downstream mechanisms of miR-133a-5p that affect IVDD, which is still unclear in our study. Finally, our study did not delve into the changes and regulation of the PFKFB2 protein. The effects of KMT2D on other physiological functions of NPCs, such as mitochondrial function and fibrosis, have not been thoroughly explored. Due to limited research funding, we were unable to compare knockdown NPCs not treated with IL-1β with the control group and investigate whether there were differences between animals of different genders. In the future, we will verify the mechanism of this experiment *in vivo*, use different animal models to assess our results regarding notochordal cells, and explore more downstream mechanisms of KMT2D and miR-133a-5p and their role in NPC degeneration, to provide theoretical knowledge of IVDD and find possible treatment directions.

In summary, our study found that KMT2D was upregulated in IL-1β-induced NPCs as a histone methyltransferase and promoted the expression of miR-133a-5p through methylation, thereby facilitating the targeted binding of miR-133a-5p to PFKFB2. The binding of miR-133a-5p to PFKFB2 reduced the mRNA level of PFKFB2, thereby inhibiting the proliferation of NPCs, promoting their apoptosis, and aggravating the degeneration of NPCs.

Acknowledgements. Not applicable.

Ethics approval and consent to participate. Animal experiments were carried out in strict accordance with the Guide for the Use of Laboratory Animals (Jones-Bolin, 2012). Animal experimental protocols were approved by the Animal Ethics Committee of the Third Affiliated Hospital of Guangzhou University of Chinese Medicine (Approval number: 2023-DSFSYYGZ102).

Consent for publication. Not applicable.

Availability of data and materials. Data will be made available upon request.

Competing interests. The authors declare that there is no conflict of interest.

Funding. There was no funding for the study.

Authors' contribution. Hongjiang Liu: conceptualization, methodology, data curation, writing-original draft, writing-review & editing; Haiquan Liu: conceptualization, data curation, formal analysis, validation; Zuyu Meng: data analysis, investigation, writing-review & editing; Wensheng Zhang: conceptualization, formal analysis, Visualization.

References

Agarwal V., Bell G.W., Nam J.W. and Bartel D.P. (2015). Predicting effective microRNA target sites in mammalian mRNAs. Elife 4, e05005.

Ang S.Y., Uebersohn A., Spencer C.I., Huang Y., Lee J.E., Ge K. and Bruneau B.G. (2016). KMT2D regulates specific programs in heart development via histone H3 lysine 4 di-methylation. Development 143, 810-821.

Boniel S., Szymanska K., Smigiel R. and Szczaluba K. (2021). Kabuki syndrome-clinical review with molecular aspects. Genes 12, 468.

Bruce J.I.E., Sanchez-Alvarez R., Sans M.D., Sugden S.A., Qi N.,

James A.D. and Williams J.A. (2021). Insulin protects acinar cells during pancreatitis by preserving glycolytic ATP supply to calcium pumps. Nat. Commun. 12, 4386.

Cao S., Li J., Yang K. and Li H. (2021). Major ceRNA regulation and key metabolic signature analysis of intervertebral disc degeneration. BMC Musculoskelet. Disord. 22, 249.

Chen Y. and Wang X. (2020). miRDB: an online database for prediction of functional microRNA targets. Nucleic. Acids. Res. 48, D127-D131.

Chen H., Wan D., Wang L., Peng A., Xiao H., Petersen R.B., Liu C., Zheng L. and Huang K. (2015). Apelin protects against acute renal injury by inhibiting TGF-β1. Biochim. Biophys. Acta 1852, 1278-1287.

Du X.F., Cui H.T., Pan H.H., Long J., Cui H.W., Chen S.L., Wang J.R., Li Z.M., Liu H., Huang Y.C., Wang H. and Zheng Z.M. (2021). Role of the miR-133a-5p/FBXO6 axis in the regulation of intervertebral disc degeneration. J. Orthop. Translat. 29, 123-133.

Fine N., Lively S., Seguin C.A., Perruccio A.V., Kapoor M. and Rampersaud R. (2023). Intervertebral disc degeneration and osteoarthritis: a common molecular disease spectrum. Nat. Rev. Rheumatol. 19, 136-152.

Francisco V., Pino J., Gonzalez-Gay M.A., Lago F., Karppinen J., Tervonen O., Mobasheri A. and Gualillo O. (2022). A new immunometabolic perspective of intervertebral disc degeneration. Nat. Rev. Rheumatol. 18, 47-60.

Froimchuk E., Jang Y. and Ge K. (2017). Histone H3 lysine 4 methyltransferase KMT2D. Gene 627, 337-342.

He J., Yang J., Shen T. and He J. (2021). Overexpression of long non-coding RNA XIST promotes IL-1β-induced degeneration of nucleus pulposus cells through targeting miR-499a-5p. Mol. Cell. Probes 57, 101711.

Ishida K., Tanishima S., Tanida A., Nagira K., Mihara T., Takeda C., Ogawa S. and Nagashima H. (2023). Comprehensive analysis of microRNA expression in lumbar facet joint capsules and synovium of patients with osteoarthritis: Comparison between early-stage and late-stage osteoarthritis samples from a single individual. J. Orthop. Sci. 29, 660-667.

Jones-Bolin S. (2012). Guidelines for the care and use of laboratory animals in biomedical research. Curr. Protoc. Pharmacol. Appendix 4, Appendix 4B.

Kang L., Zhang H., Jia C., Zhang R. and Shen C. (2023). Epigenetic modifications of inflammation in intervertebral disc degeneration. Ageing Res. Rev. 87, 101902.

Kim M., Yi S.A., Lee H., Bang S.Y., Park E.K., Lee M.G., Nam K.H., Yoo J.H., Lee D.H., Ryu H.W., Kwon S.H. and Han J.W. (2014). Reversine induces multipotency of lineage-committed cells through epigenetic silencing of miR-133a. Biochem. Biophys. Res. Commun. 445, 255-262.

Kim D.H., Kim J., Kwon J.S., Sandhu J., Tontonoz P., Lee S.K., Lee S. and Lee J.W. (2016). Critical roles of the histone methyltransferase MLL4/KMT2D in murine hepatic steatosis directed by ABL1 and PPARgamma2. Cell Rep. 17, 1671-1682.

Kos N., Gradisnik L. and Velnar T. (2019). A brief review of the degenerative intervertebral disc disease. Med. Arch. 73, 421-424.

Li Z., Yang H., Hai Y. and Cheng Y. (2023). Regulatory effect of inflammatory mediators in intervertebral disc degeneration. Mediators Inflamm. 2023, 6210885.

Livak K.J. and Schmittgen T.D. (2001). Analysis of relative gene expression data using real-time quantitative PCR and the 2(-Delta Delta C(T)) Method. Methods 25, 402-408.

Miranda K.C., Huynh T., Tay Y., Ang Y.S., Tam W.L., Thomson A.M., Lim B. and Rigoutsos I. (2006). A pattern-based method for the identification of MicroRNA binding sites and their corresponding heteroduplexes. Cell 126, 1203-1217.

Molladavoodi S., McMorran J. and Gregory D. (2020). Mechanobiology of annulus fibrosus and nucleus pulposus cells in intervertebral discs. Cell Tissue Res. 379, 429-444.

Piletič K. and Kunej T. (2016). MicroRNA epigenetic signatures in human disease. Arch. Toxicol. 90, 2405-2419.

Qi S., Li C., Kong X. and Zheng Q. (2020). Dexmedetomidine suppresses oxidative stress and inflammation of nucleus pulposus cells by activating the PI3K/Akt signaling pathway. Pharmazie 75, 505-509.

Rider M.H., Bertrand L., Vertommen D., Michels P.A., Rousseau G.G. and Hue L. (2004). 6-phosphofructo-2-kinase/fructose-2,6-bisphosphatase: head-to-head with a bifunctional enzyme that controls glycolysis. Biochem. J. 381, 561-579.

Risbud M.V. and Shapiro I.M. (2014). Role of cytokines in intervertebral disc degeneration: pain and disc content. Nat. Rev. Rheumatol. 10, 44-56.

Saliminejad K., Khorram Khorshid H.R., Soleymani Fard S. and Ghaffari S.H. (2019). An overview of microRNAs: Biology, functions, therapeutics, and analysis methods. J. Cell. Physiol. 234, 5451-5465.

Sato F., Tsuchiya S., Meltzer S.J. and Shimizu K. (2011). MicroRNAs and epigenetics. FEBS J. 278, 1598-1609.

Shen E., Shulha H., Weng Z. and Akbarian S. (2014). Regulation of histone H3K4 methylation in brain development and disease. Philos. Trans. R. Soc. Lond. B Biol. Sci. 369, 20130514.

Shinsky S.A., Monteith K.E., Viggiano S. and Cosgrove M.S. (2015). Biochemical reconstitution and phylogenetic comparison of human SET1 family core complexes involved in histone methylation. J. Biol. Chem. 290, 6361-6375.

Sticht C., De La Torre C., Parveen A. and Gretz N. (2018). miRWalk: An online resource for prediction of microRNA binding sites. PLoS One 13, e0206239.

Tian X., Li L., Fu G., Wang J., He Q., Zhang C., Qin B. and Wang J. (2021). miR-133a-3p regulates the proliferation and apoptosis of intestinal epithelial cells by modulating the expression of TAGLN2. Exp. Ther. Med. 22, 824.

Wang Z., Wei D., Bin E., Li J., Jiang K., Lv T., Mao X., Wang F., Dai H. and Tang N. (2023). Enhanced glycolysis-mediated energy production in alveolar stem cells is required for alveolar regeneration. Cell Stem Cell 30, 1028-1042.e7.

Wu A., March L., Zheng X., Huang J., Wang X., Zhao J., Blyth F.M., Smith E., Buchbinder R. and Hoy D. (2020). Global low back pain prevalence and years lived with disability from 1990 to 2017: estimates from the Global Burden of Disease Study 2017. Ann. Transl. Med. 8, 299.

Wu L., Shen J., Zhang X. and Hu Z. (2021). LDHA-Mediated glycolytic metabolism in nucleus pulposus cells is a potential therapeutic target for intervertebral disc degeneration. Biomed. Res. Int. 2021, 9914417.

Xin J., Wang Y., Zheng Z., Wang S., Na S. and Zhang S. (2022). Treatment of intervertebral disc degeneration. Orthop. Surg. 14, 1271-1280.

Xu W., Zhang X., Liu G., Zhu M., Wu Y., Jie Z., Xie Z., Wang S., Ma Q., Fan S. and Fang X. (2020). Oxidative stress abrogates the degradation of KMT2D to promote degeneration in nucleus

pulposus. Biochim. Biophys. Acta Mol. Basis. Dis. 1866, 165888.
Yuan X., Li T., Shi L., Miao J., Guo Y. and Chen Y. (2021). Human umbilical cord mesenchymal stem cells deliver exogenous miR-26a-5p via exosomes to inhibit nucleus pulposus cell pyroptosis through METTL14/NLRP3. Mol. Med. 27, 91.
Zhang G.Z., Liu M.Q., Chen H.W., Wu Z.L., Gao Y.C., Ma Z.J., He X.G. and Kang X.W. (2021). NF-κB signalling pathways in nucleus pulposus cell function and intervertebral disc degeneration. Cell Prolif. 54, e13057.
Zhao Y. and Ai Y. (2020). Overexpression of lncRNA Gm15621 alleviates apoptosis and inflammation response resulting from sevoflurane treatment through inhibiting miR-133a/Sox4. J. Cell. Physiol. 235, 957-965.
Zhao Y. and Li A. (2021). miR-19b-3p relieves intervertebral disc degeneration through modulating PTEN/PI3K/Akt/mTOR signaling pathway. Aging (Albany NY). 13, 22459-22473.

Accepted September 12, 2024